Revealing the new structure of B_8N_8 nanocage and comparison of hydrogen storage capacity

Vesim Nasif, Koray Sayin [*]

Department of Chemistry, Faculty of Science, Sivas Cumhuriyet University, 58140 Sivas, Turkey

ARTICLE INFO

ABSTRACT

The new structure for B_8N_8 nanocage was revealed. This structure is completely different from the known structure. The structural properties of investigated structures were investigated and compared with each other. The new structure of B_8N_8 nanocage was characterized by IR and NMR spectrum. The size of known and new structure of B_8N_8 nanocage was determined as 42.63 and 43.80 nm, respectively. Electronic properties of structure of BN nanocage are investigated. Finally, hydrogen storage capacity is investigated and it can be said that the DOE target may be reached by the new structure of B_8N_8 nanocage.

1. Introduction

Carbon nanomaterials, for instance fullerene, nanotubes, nanocapsules, nanospring and onions have a wide application area [1–4]. However, carbon nanomaterials have significant disadvantages and they limit the application area. Carbon nanomaterials are degraded at 600 °C and do not have sufficient thermal stability while boron nitrite nanomaterials can withstand up to high temperature and have well thermal conductivity [5]. There are a lot of studies about B_xN_x (x > 12) in literature but there are limited studies on B_8N_8 nanocage [6–10]. Furthermore, the point group of B_8N_8 has been reported as S_4 but the reported studies have not been encountered in the literature. BN nanomaterials have a lot of application industries [11].

There are many energy sources, including renewable and fossil fuels, that human beings can use. One of the clean and renewable energy sources is hydrogen energy. However, hydrogen energy is not a primary source. Initially, hydrogen must be produced using energy from another source and then transported for usage. Hydrogen can be obtained from diverse resources such as hydro, wind, wave, solar, biomass, geothermal, coal, natural gas and nuclear. Hydrogen is clean energy due to the fact that water releases when the hydrogen is burnt. Because of that the ability of hydrogen to replace fossil fuels in the transportation sector could address one of the world's major environmental problems. It has been known that the automotive industry is one of the main factors polluting the world [12].

There is a lot of production methods for hydrogen such as splitting water through various processes, including electrolysis and etc. However, the main problems of the usage of hydrogen energy are storage and transporting. Although there are a lot of storage material, hydrogen has very low energy density per unit volume due to the lightest chemical element. Also, hydrogen can be transport nanomaterials which are based on carbon (C) and boron nitrite (BN) structures. But, there are a lot of advantages of BN nanomaterials such as high temperature resistance, broad application areas, etc. As for the nanostructures, there are a lot structure such as cage/fullerene, solid cluster, onion, tube. In this study, BN nanocages are considered as nanomaterial for the carrying of hydrogen.

In previous studies, BN nanocages have been investigated in many papers. The storage capacity (wt. %) is found as 1.35, 3.05, 4.96, 6.60 and 10.58 for $B_{12}N_{12}$, $B_{24}N_{24}$, $B_{36}N_{36}$, $B_{48}N_{48}$ and $B_{96}N_{96}$ [13]. These nanocages are investigated at PM7 method. The hydrogen are stored to BN nanocage by chemisorption. BN nanotubes are synthesized and characterized by Okan et al. in 2012 [14]. In synthesis, different catalysts have been used in their study and the maximum hydrogen storage capacity has been found as 0.85 wt% [14]. BN nanotube ($B_{99}N_{99}$) and nanocapsule ($B_{36}N_{36}$) have been synthesized by Oku and co-workers in 2004. Characterization of the related structures have been done by using different techniques. In their study, hydrogen storage capacity has been found as ~3 wt% [15]. $B_{12}N_{12}$ nanoclusters have been investigated by Janjua in 2021. Different alkaline earth metals have been used. All calculations have been performed at B3LYP/6-31G(d,p) and CAM-B3LYP/6-311+G(d,p) levels. Adsorption energy of hydrogen molecule has been calculated as −1.06 kJ/mol [16]. According to above studies, hydrogen storage of BN nanomaterial have been investigated as both experimentally and computationally.
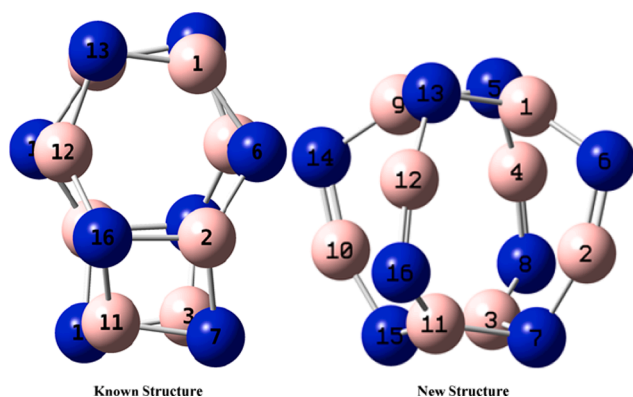
Although double-hybrid DFT and low-level composite *ab-initio*

Table 1
Thermodynamic parameters of isomeric structure of B_8N_8 nanocage.

Isomers	Point Group	Gas Phase			Water		
		E_{Total}[a]	H[a]	G[a]	E_{Total}[a]	H[a]	G[a]
Known Structure	C_1	-1.67117×10^6	-1.67116×10^6	-1.67127×10^6	-1.67120×10^6	-1.67119×10^6	-1.67129×10^6
	C_2	-1.67117×10^6	-1.67116×10^6	-1.67127×10^6	-1.67119×10^6	-1.67119×10^6	-1.67113×10^6
	C_{2v}	–	–	–	–	–	–
	D_2	–	–	–	–	–	–
	D_{2d}	–	–	–	–	–	–
	S_4	-1.67117×10^6	-1.67116×10^6	-1.67127×10^6	-1.67119×10^6	-1.67119×10^6	-1.67129×10^6
New Structure	C_1	-1.67120×10^6	-1.67119×10^6	-1.67131×10^6	-1.67122×10^6	-1.67122×10^6	-1.67133×10^6
	C_2	-1.67120×10^6	-1.67119×10^6	-1.67131×10^6	-1.67122×10^6	-1.67122×10^6	-1.67133×10^6
	C_{2v}	-1.67120×10^6	-1.67119×10^6	-1.67131×10^6	-1.67122×10^6	-1.67122×10^6	-1.67133×10^6
	D_2	-1.67120×10^6	-1.67119×10^6	-1.67131×10^6	-1.67122×10^6	-1.67122×10^6	-1.67133×10^6
	D_{2d}	-1.67120×10^6	-1.67119×10^6	-1.67131×10^6	-1.67122×10^6	-1.67122×10^6	-1.67133×10^6
	S_4	-1.67120×10^6	-1.67119×10^6	-1.67131×10^6	-1.67122×10^6	-1.67122×10^6	-1.67133×10^6

[a] in kJ/mol

Fig. 1. The optimized structure of known and new structure of B_8N_8 nanocage with atomic labeling.

Table 2
The calculated geometric parameters.

Assignments	Known Structure		New Structure	
	Gas Phase	Water	Gas Phase	Water
Bond Lengths (Å)				
B1 - N6	1.470	1.469	1.408	1.410
B1 - N13	1.474	1.475	1.506	1.506
B2 - N6	1.454	1.454	1.295	1.297
B2 - N16	1.512	1.511	–	–
B2 - N7	1.479	1.481	1.391	1.390
B11 - N7	1.489	1.490	1.507	1.506
B11 - N16	1.470	1.469	1.408	1.410
B12 - N16	1.454	1.454	1.295	1.297
B12 - N13	1.479	1.481	1.391	1.390
Bond Angle (deg.)				
N6 - B1 - N13	129.6	129.5	129.0	129.0
N6 - B2 - N7	124.7	124.6	159.6	159.0
N6 - B2 - N16	123.3	123.3	–	–
B1 - N6 - B2	113.1	113.2	107.9	107.7
B2 - N7 - B11	78.0	78.0	107.5	108.0
N7 - B11 - N16	101.2	101.1	129.0	129.0
N13 - B12 - B16	124.7	124.6	159.7	159.1
B2 - N16 - B11	77.5	77.7	–	–
B2 - N16 - B12	105.9	106.0	–	–

methods present better calculations results such as optimization structure and energy values for BN nanocage, the whole calculations are performed at PBE1PBE/6-311+G(d) in gas phase and water in this study. DFT methods has been extensively benchmarked for energetic properties [17–19]. The most used DFT methods were examined by

Goerigk et al. in 2017; by Mardirossian and Head-Gordon in 2017 and by Karton and Spackman in 2021 and it was reported that the PBE1PBE method chosen in this study was neither the best nor the worst in performance. It is indirectly stated that the DFT method used in this study has an average performance and can be used in energy calculations [17–19]. Six different point groups, C_1, C_2, C_{2v}, D_2, D_{2d} and S_4, are taken into consideration. Additionally, a new structure has been observed from the calculations results. Then, structural, properties and electronic properties belong to known and new structures are compared each other. The point group of B_8N_8 nanocage in gas phase and water is determined as C_1 and C_2, respectively. The geometric parameters of structures are found as different from each other. Especially, some B-N bonds are found as shorter in new structure. As for the spectral characterization of the new structure of B_8N_8 nanocage, stretching frequencies for BN bond are observed in two regions which are nearly 1400 and 1900 cm^{-1}. It implies that there are two bonds between some B-N bonds. In addition to IR spectrum, NMR spectrum is calculated and the NMR results are supported the structural and IR results. The decomposition temperatures are calculated as ~1450 °C and ~1180 °C for known and new structures, respectively. Actually, two structures are isomers each other and transition state, therefore, is calculated in gas phase and water. Moreover, the transition temperatures from the old to the new structure are also calculated as 931 and 842 °C for the gas and water phase, respectively. All these temperature researches, thermodynamic parameters are used. These results show that the old one transitions at 931 °C to new one and it means that B_8N_8 nanocage is stable up to ~1180 °C. Finally, hydrogen storage capacity of the both isomers is investigated at same level of theory. The hydrogen storage capacity of new structure is calculated as 9.14% while it is 1.01% for known structure. As a result, the hydrogen storage capacity is seemed as excellent and it is envisaged that the DOE's goal has been achieved and improved.

2. Method

The computational researchers were done by using Gaussian programs, ChemOffice [20–23]. Numerical calculations and preparation of input file were done by Gaussian programs while ChemOffice was used to preparation of figures for the article. In this project, PBE1PBE which is one of the hybrid density functional theory (DFT) functions and 6-311+G(d) basis set were used due to the fact that the related method and basis set have been used for BN nanocage [24–28]. For solute – solvent interactions, conductor like polarized continuum model (C-PCM) was used and transition state was calculated by using QST2 method [29]. Heat capacity of studied compounds was used to calculate the decomposition and transition temperatures. To compare electronic properties, molecular orbital energy diagram (MOED), contour diagram of frontier molecular orbitals (FMOs), molecular electrostatic potential (MEP)
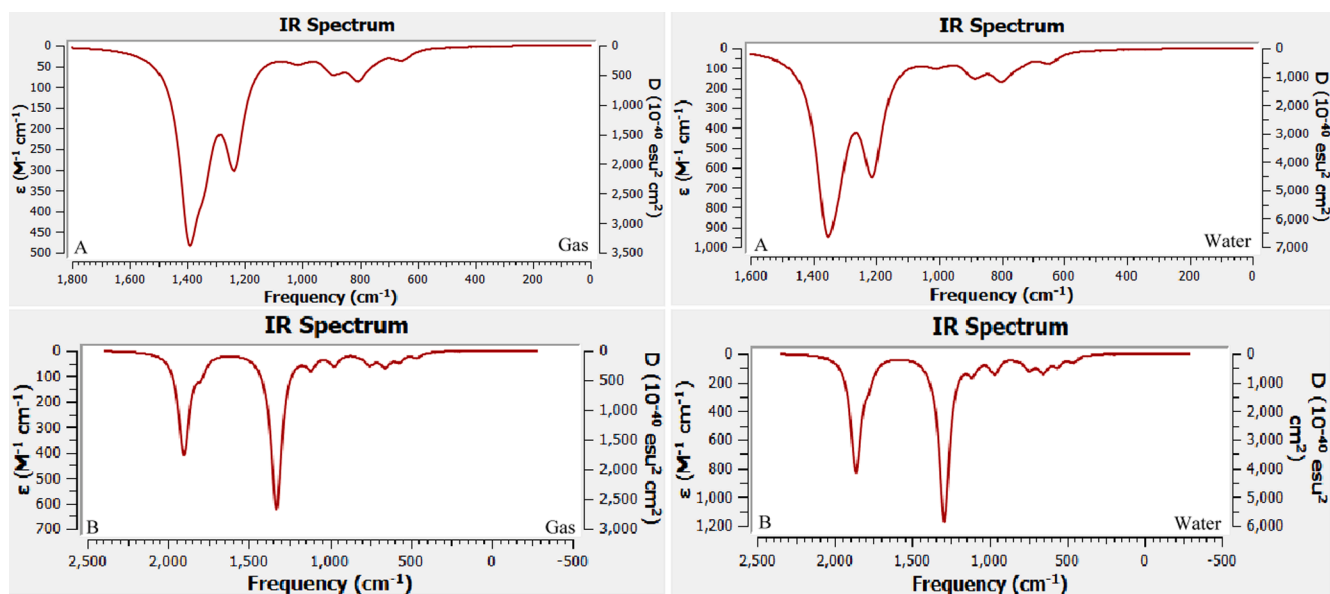
Fig. 2. Calculated IR spectrum of known (A) and new (B) structures of B_8N_8 nanocage at PBE1PBE/6-311+G(d) level.

Table 3
Chemical shift values (ppm) of boron and nitrogen atoms in the mentioned B_8N_8 nanocages.

Assignment	Known Structure		New Structure	
	Gas	Water	Gas	Water
B1	33.8	33.9	35.5	35.7
B2	33.6	33.6	27.8	28.2
B3	33.8	33.9	35.5	35.7
B4	33.6	33.7	27.8	28.2
N5	200.1	196.4	137.0	138.3
N6	147.2	146.8	162.5	158.6
N7	200.0	196.4	137.1	138.3
N8	147.3	146.8	162.5	158.6
B9	33.8	33.9	35.5	35.7
B10	33.6	33.6	27.8	28.2
B11	33.8	33.9	35.5	35.7
B12	33.6	33.7	27.8	28.2
N13	200.1	196.4	137.0	138.3
N14	147.2	146.8	162.5	158.6
N15	200.0	196.4	137.1	138.3
N16	147.3	146.8	162.5	158.6

maps were calculated. Finally, hydrogen storage capacity is investigated at PBE1PBE/6-311+G(d) level in gas phase.

3. Results and discussions

3.1. Geometric structure at ground state

Symmetry point group is important to determine the chemical and spectral properties of related compounds. B_xN_x (x = 8) has been investigated in literature [30]. Although structure and symmetry point group of B_8N_8 have been identified, a detailed article in which these studies have been conducted has not been found. Geometric structure and chemical properties of B_8N_8 nanocage are investigated in detail at PBE1PBE/6-311+G(d) level in gas and water via taking into consideration of C_1, C_2, C_{2v}, D_2, D_{2d} and S_4 point groups. However, the calculation errors are encountered at C_{2v}, D_2, D_{2d} and S_4 point groups in the optimization of the known (old) structure of B_8N_8 nanocage. An unknown structure of B_8N_8 is observed at the result of calculations. Thermodynamic parameters, total energy (E_{Total}), enthalpy (H) and Gibbs Free energy (G), are given in Table 1 for known and new structures in

each point group.

According to Table 1, point group of the most stable structure is calculated as C_1 and C_2 for gas phase and water in the known and new structures, respectively. In literature, the point group of known structure has been reported as S_4. However, this datum is proven to be completely false by this study. As for the stable structure, new structure is about 29 kJ/mol more stable than the that of known structure. The optimized structures of both isomers are given in Fig. 1. It can be said that chemical properties of new structure may be more attractive than that of known structure due to the double bonds. Additionally, the geometric parameters are given in Table 2.

Actually, the bond lengths are similar to each other except some bonds. Some bonds which are B2-N6, B2-N16, B10-N8 and B10-N16, are broken. Furthermore, B2-N6, B4-N8, B10-N14 and B12-N16 are shortened from 1.454 Å to 1.29 Å. These bonds seem as double bond at the result of calculations. According to obtained results, it is expected that new structure of B_8N_8 exhibits different molecular and chemical properties than that of the known structure.

3.2. Spectral characterization

Characterization of compounds structure is so important for further analysis. Many spectral techniques such as infrared (IR), nuclear magnetic resonance (NMR) spectroscopy and etc. can be used for this aim. Infrared and nuclear magnetic resonance spectrum are so important in the determination of atom type, number and functional groups. Functional groups such as hydrogen bonds, aromatic groups and etc. can be determined by IR spectrum while detail of molecular structure can be determined via NMR spectrum. IR spectrum for mentioned B_8N_8 nano structures are calculated and represented in Fig. 2.

The stretching frequency of B-N bond is calculated nearly 1350 cm^{-1} in each spectrum. As experimentally, B-N bond has been observed at nearly 1380 cm^{-1} [31,32]. The calculated vibrational frequency for B-N bond in known structure is in a good agreement with experimental results. However, there is a different peak in IR spectrum of new structure. The frequency of this peak is observed about 1900 cm^{-1}. This peak is in the double bond region. Additionally, vibrational frequency of B = C/B = N has been observed nearly 1780 cm^{-1} [33,34]. Computational results are in agreement with experimental data. So, it can be said that there is a double bond (B = N) in new structure. ^{11}B NMR and ^{15}N NMR are calculated and chemical shift values of related atoms are given in Table 3.
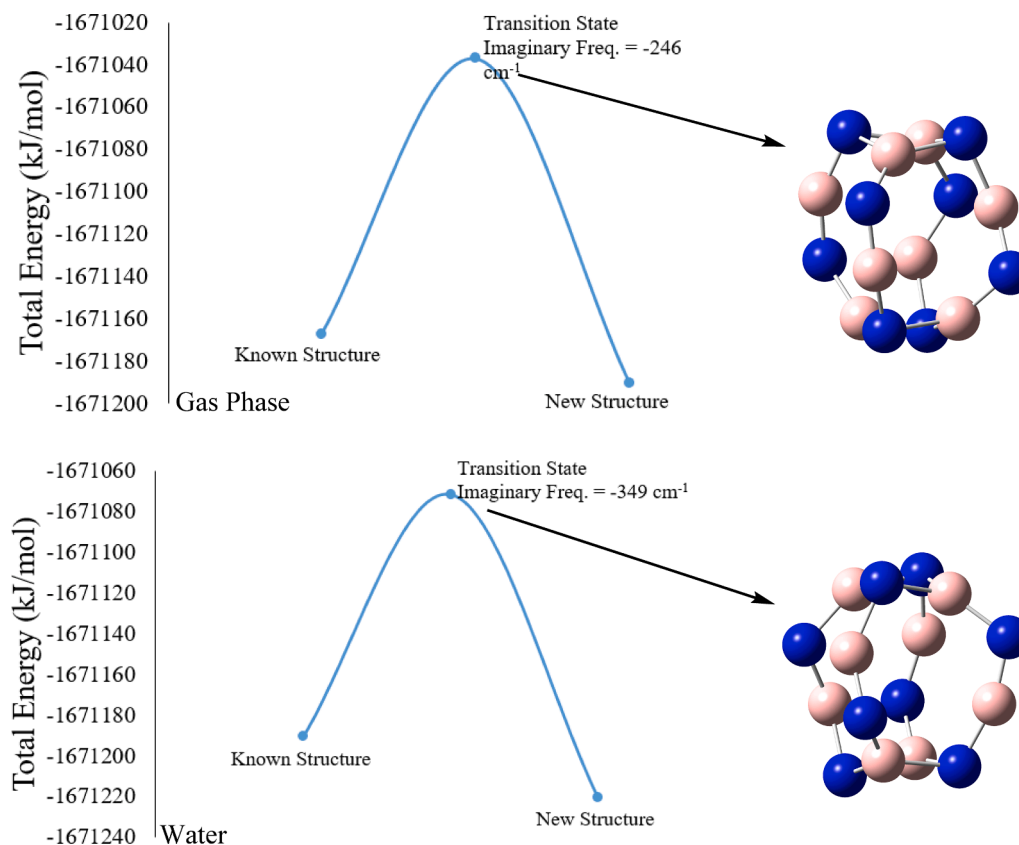
Fig. 3. The transition state structures, imaginary frequencies and energy diagram of mentioned B_8N_8 nanocage.

Table 4
NBO charges of boron and nitrogen atoms on B_8N_8 structures.

Assignment	Known Structure		New Structure	
	Gas Phase	Water	Gas Phase	Water
B1	1.026	1.043	1.113	1.122
B2	1.151	1.160	1.161	1.178
B3	1.026	1.043	1.113	1.122
B4	1.151	1.160	1.161	1.178
N5	−1.035	−1.054	−1.175	−1.179
N6	−1.142	−1.150	−1.099	−1.121
N7	−1.035	−1.054	−1.175	−1.179
N8	−1.142	−1.150	−1.099	−1.121
B9	1.026	1.043	1.113	1.122
B10	1.151	1.160	1.161	1.178
B11	1.026	1.043	1.113	1.122
B12	1.151	1.160	1.161	1.178
N13	−1.035	−1.054	−1.175	−1.179
N14	−1.142	−1.150	−1.099	−1.121
N15	−1.035	−1.054	−1.175	−1.179
N16	−1.142	−1.150	−1.099	−1.121

According to Table 3, the chemical shift values of boron and nitrogen atoms are different from each other which can be seen easily from related table. Especially, the chemical shift values of N5, N7, N13 and N15 are significant. In these atoms, they gave a peak at lower ppm due to the high shielding effect. So, these values imply that these structures are different from each other.

3.3. Defining the transition state (TS)

Transition state is so important in the determination of reaction and transition mechanism. In this step, QST2 method is used in the computational analyses. The transition state between known and new structure of B_8N_8 nanocage is investigated in gas phase and water. The

energy diagram and structure of TS are represented in Fig. 3.

According to Fig. 3, the imaginary frequency for gas and water is calculated as −349 and −246 cm^{-1}, respectively. These frequencies are in the acceptable range for transition state [35,36]. It can be easily seen that some bonds are breaking and some bonds are being stronger and molecular structures both of them are completely different from each other. Additionally, how they are transition from each other can be seen from this figure. Finally, it can be said that the new structure of related nanocage is more stable than the known one due to the energy of them and the geometric structure of new one is like ball than that of other one. The new structure is more like fullerene.

3.4. Comparing the electronic properties

In this section, natural bond orbital (NBO) charge, molecular orbital energy diagram (MOED), contour diagram of frontier molecular orbital and molecular electrostatic potential (MEP) maps are investigated in detail and electrophilic/nucleophilic attack region are determined using these results. NBO charges of boron and nitrogen atoms are calculated and the results are given in Table 4.

According Table 4, the charges are mainly same to each other. However, there are some differences. For instance, the charge of B1 and B3 is +1.026 in known structure while it is +1.113 in new structure. As for the nitrogen atoms, the charge of N5 and N7 is changing from −1.035 to −1.175. It can be seen so small changes but it may affect the electronic and chemical properties. The MOED of B_8N_8 structures are calculated and represented in Fig. 4.

According to Fig. 4, the frontier molecular orbitals of known structures are HOMO-3, HOMO-2, HOMO-1, HOMO, LUMO, LUMO + 1, LUMO + 2 and LUMO + 3. Since, HOMO-3 – HOMO are equal energy while LUMO – LUMO + 3 are same, too. Additionally, HOMO of new structure is one of the frontier molecular orbital while LUMO, LUMO + 1, LUMO + 2 and LUMO + 3 are frontier molecular orbitals for new
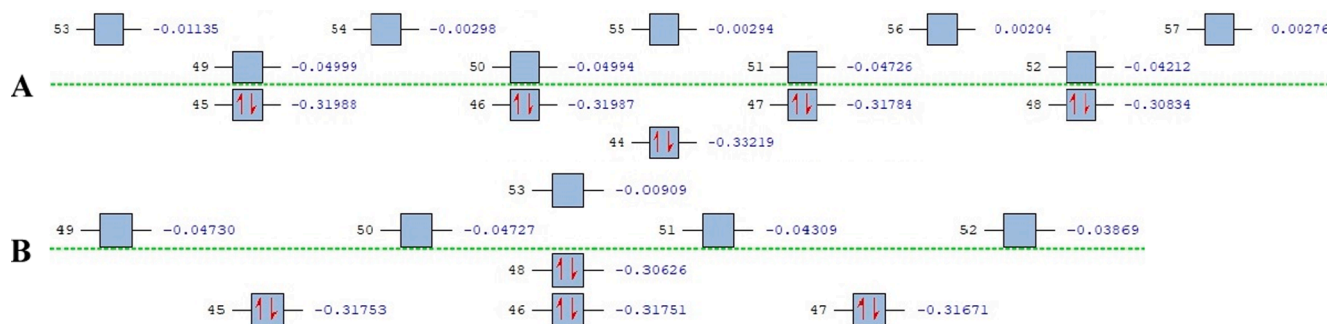
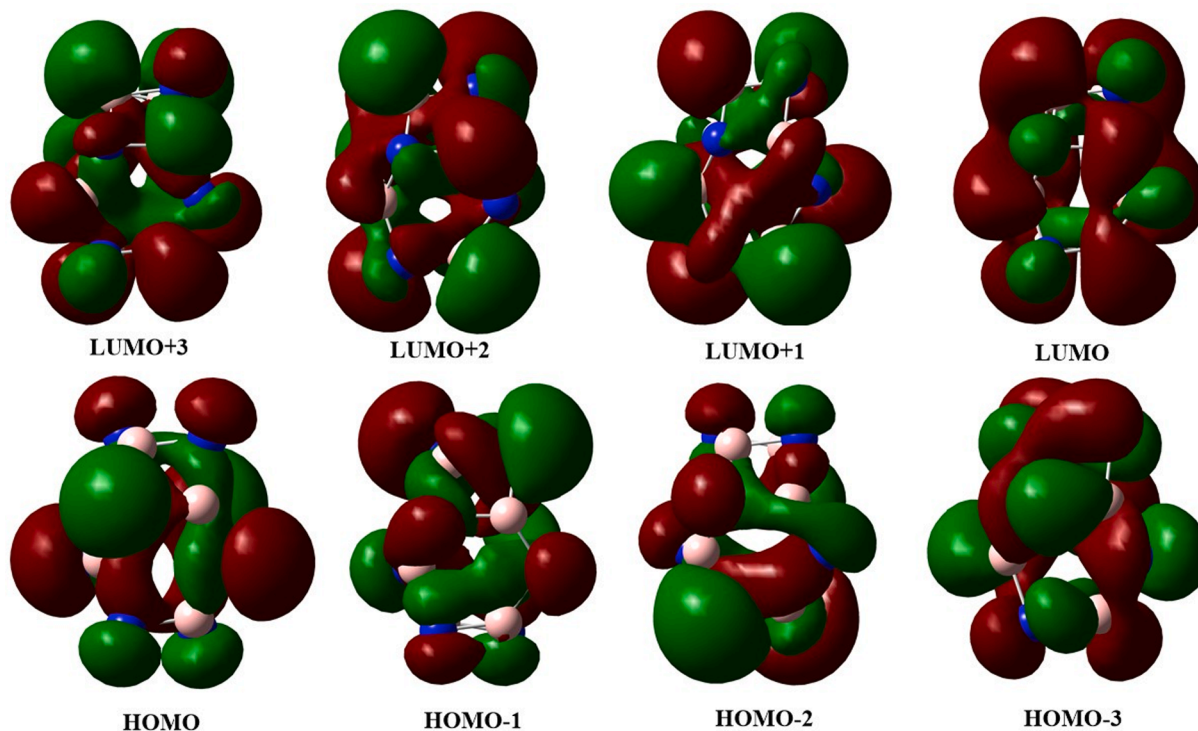**Fig. 4.** MOED of known (A) and new (B) structure of B_8N_8 nanocage.

Fig. 5. Contour plots of frontier molecular orbital of known structure.

structure of BN nanocage. The contour plots of these molecular orbitals are represented in Figs. 5 and 6 for known and new structures, respectively.

According to Figs. 5 and 6, there are balloon environment of nitrogen and boron atoms in both occupied and unoccupied molecular orbitals. There are two electrons in occupied molecular orbitals while no electron in unoccupied molecular orbitals. The electrons mainly localize on nitrogen atom in occupied MO while the balloons are mainly localized on the environment of boron atom. Finally, molecular electrostatic potential (MEP) maps are calculated for each structure and represented in Fig. 7.

According to Fig. 7, the electron rich and poor regions are more distinct and clearly separated from each other in new structure. Due to the fact that chemical properties may better than that of known structure.

3.5. Investigation of hydrogen storage capacity

Hydrogen energy is so important for human and one of the renewable energies. Hydrogen energy attracts the attention of many countries and many investments have been done by many countries. Especially,

many car companies are investing in hydrogen energy. There are three steps for hydrogen energy which are production, storage and transportation. In this study, B_8N_8 nanocages are taken into account for storage and transportation. The storage target in nanomaterial is determined as 6.5% (w/w) by Department of Energy (DOE) of U.S.A. There is no data about storage capacity of B_8N_8 in literature. The storage capacity of known and new structure of related BN nanocage are investigated at PBE1PBE/6-311+G(d) level in gas phase. BN nanocages are optimized by adding the hydrogen molecule one by one.

In the known structure of B_8N_8, only one hydrogen molecule is storage. As for the second one, the nanocage is shattered in trying to second storage of H_2. These structures are given in Fig. 8.

According to this result, only one hydrogen molecule is storage to related BN nanocage. The storage percentage is calculated as 1.01% and the adsorption energy is calculated as 846.99 kJ/mol. For the known structure, it is not efficient for the storage and transportation. Because, only one hydrogen molecule is storage and the desorption of it is impossible. Therefore, known structure cannot be preferred for the hydrogen energy.

As for the new structure, hydrogen molecules are tried to storage inside of the nanocage. The first molecule is storage to inside of
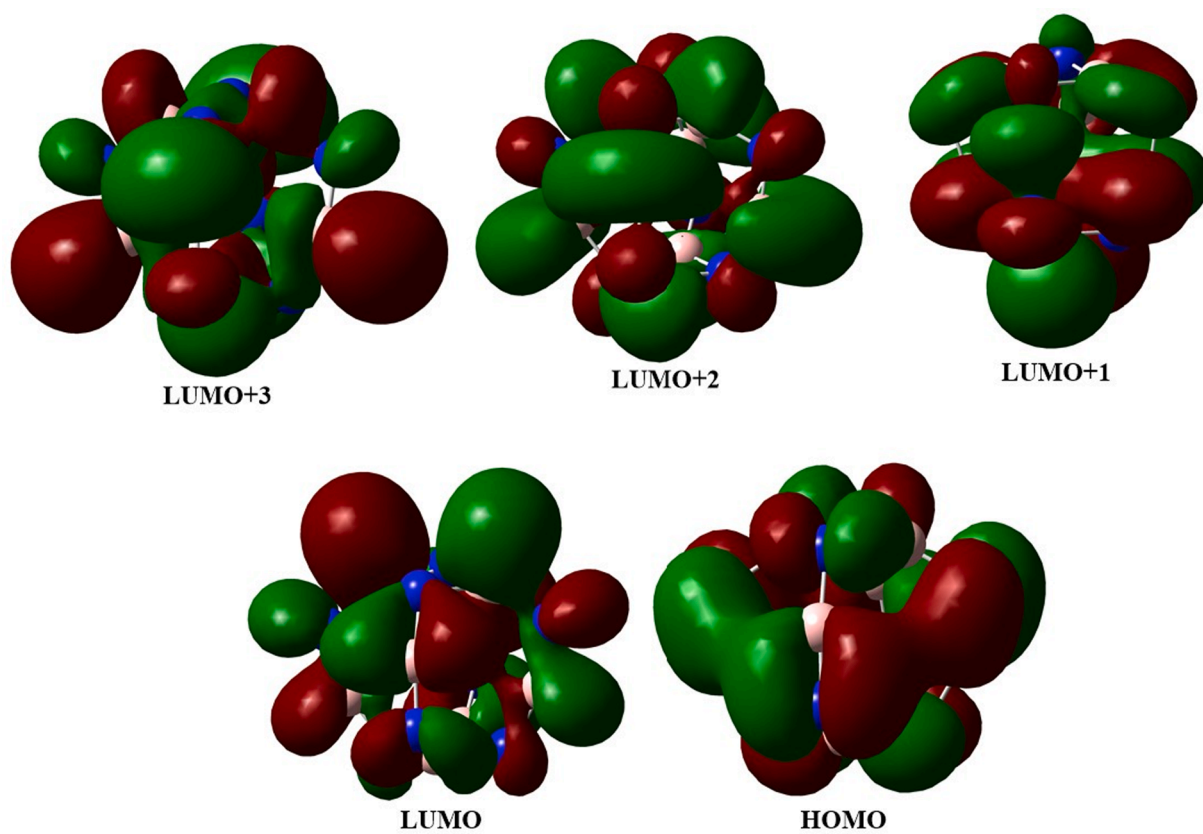
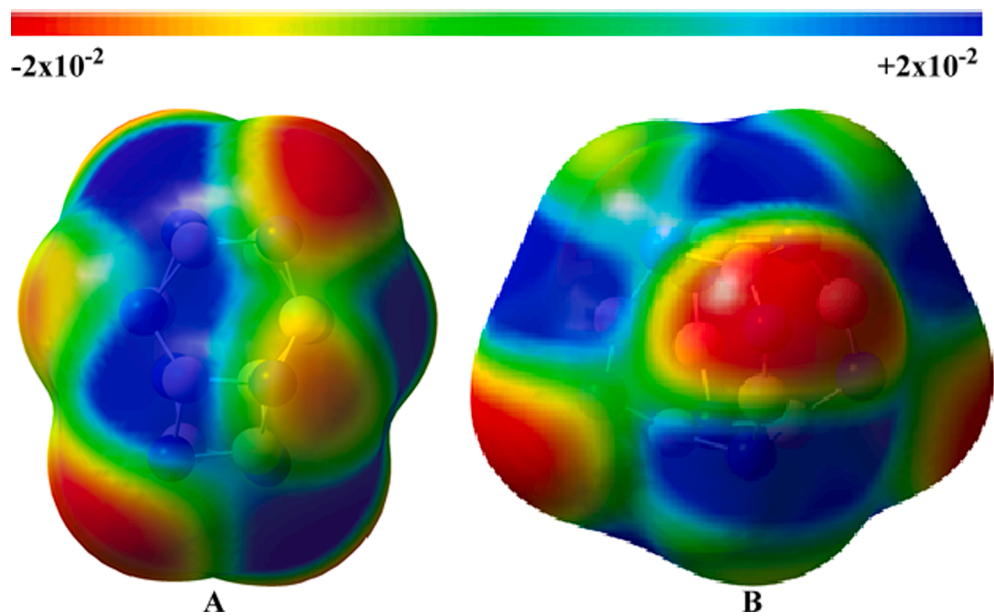**Fig. 6.** Contour plots of frontier molecular orbital of new structure.

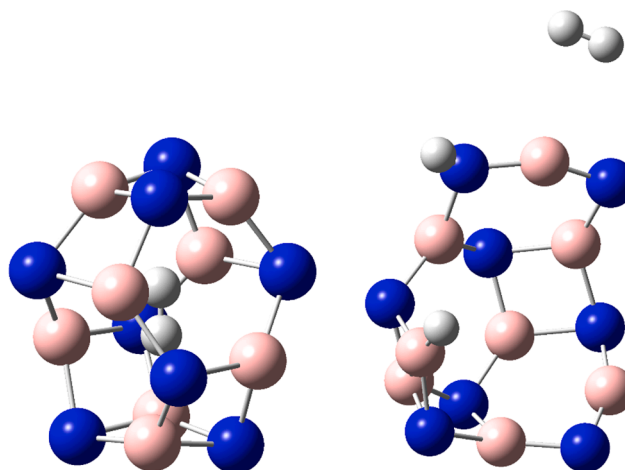**Fig. 7.** MEP maps of known (A) and new (B) structure of BN nanocage.

Fig. 8. The optimized structure of the known BN nanocage with hydrogen molecule.

nanocage. However, the second and the other hydrogen molecules are clinged to outside of the nanocage although the hydrogen molecules is put the inside of the nanocage. So, nine hydrogen molecules is storaged on the new structure of B_8N_8. Some optimized structures are represented in Fig. 9.

According to Fig. 9, the first hydrogen molecule is storaged to inside of the nanocage and probably its desorption is to hard in the production of energy. However, the other hydrogen molecules are clinged to outside of the related BN nanocage. Hydrogen molecules can be easily desorption from the related nanocage to product the energy. This would be more efficient for the aim. The average distance between H_2 and nanocage is nearly 2.99 Å. Additionally, it is seen that hydrogen molecules interact with boron atoms at nanocage. It can be said that the boron atoms provide extra property to inorganic fullerene for the storage of hydrogens. As for the DOE target, The storage efficiency is calculated as 9.14% and the adsorption energy per hydrogen molecule is given in Table 5.

According to Fig. 9 and Table 5, the storage capacity of new structure of B_8N_8 nanocage is better than the other one. In addition to storage, desorption investigations are also investigated by the MM2 method. As a result, there is no released H_2 molecule in the known structure while eight H_2 molecules are released from the new structure. We found that the hydrogen molecule trapped in the cage is never released. For desorption of the hydrogen molecule, the cage must be broken down. In this way, the cage cannot be reused. All of these reasons, the known structure of B_8N_8 cannot be used for hydrogen energy. As for the new structure of it, storage efficiency is calculated as 9.14% while desorption efficiency is calculated as 88.9% which is related with storage hydrogen molecules. Furthermore, this nanocage can be used over and over. Finally, the target of DOE can be reached by this structure.

4. Conclusions

B_8N_8 nanocage was optimized at PBE1PBE/6-311+G(d) level in gas phase and water. In the optimization, symmetry point group was taken into account. The new structure for mentioned nanocage is encountered. The structural and electronic properties of B_8N_8 nanocages were examined in detail. Additionally, B_8N_8 structures were characterized by IR and NMR spectrum. The size of known and new structure of B_8N_8 nanocage was determined as 42.63 and 43.80 nm, respectively. Especially, hydrogen storage capacity of the known and new structures was investigated. The storage capacity is determined as 1.01% and 9.14% for the known and new structure of BN nanocage, respectively. All results showed that the DOE target may be reached by new structure of B_8N_8 nanocage.

Table 5
The adsorption energy (kJ/mol) per H_2 molecule.

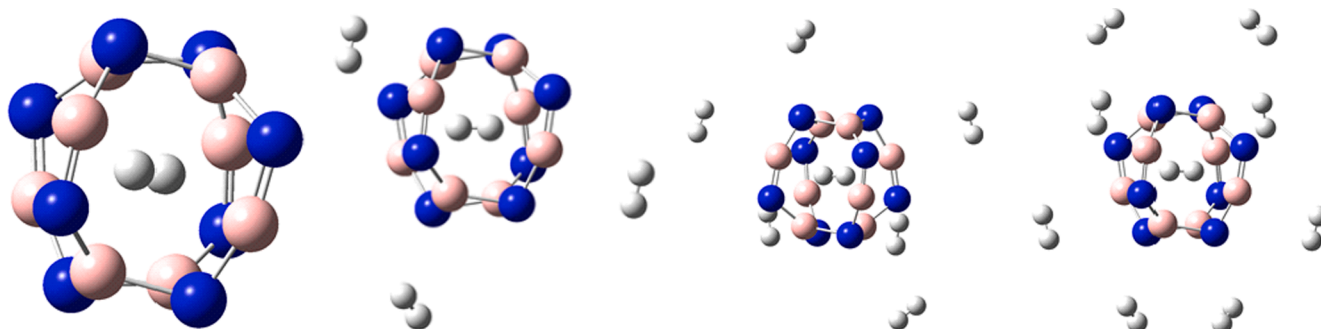| Number of H_2 Molecule	Adsorption Energy[a]	Number of H_2 Molecule	Adsorption Energy[a]
1	478.1	6	84.1
2	242.4	7	72.6
3	42.0	8	64.2
4	123.6	9	57.5
5	99.9	–	–

[a] for per H_2 molecule.

Fig. 9. The hydrogen storaged new B_8N_8 nanocage.

Declaration of Competing Interest

The authors declare that they have no known competing financial interests or personal relationships that could have appeared to influence the work reported in this paper.

Acknowledgments

References

[1] S. Iijima, Helical microtubules of graphitic carbon, Nature 354 (6348) (1991) 56–58.

[2] R.T. Yang, Hydrogen storage by alkali-doped carbon nanotubes–revisited, Carbon 38 (2000) 623–625.

[3] M. Ritschel, M. Uhlemann, O. Gutfleisch, A. Leonhardt, A. Graff, C.h. Taschner, J. Fink, Appl. Phys. Lett. 80 (2002) 2985–2987.

[4] H. Kajiura, S. Tsutsui, K. Kadono, M. Kakuta, M. Ata, Y. Murakami, Hydrogen storage capacity of commercially available carbon materials at room temperature, Appl. Phys. Lett. 82 (7) (2003) 1105–1107.

[5] Q. Sun, Q. Wang, P. Jena, Storage of molecular hydrogen in B-N cage: energetics and thermal stability, Nano Lett. 5 (7) (2005) 1273–1277.

[6] T. Oku, A. Nishiwaki, I. Narita, Formation and atomic structures of BnNn (n = 24–60) clusters studied by mass spectrometry, high-resolution electron microscopy and molecular orbital calculations, Physica B 351 (2004) 184.

[7] Y.-C. Zhu, Y. Bando, L.-W. Yin, D. Golberg, Hollow boron nitride (BN) nanocages and BN-nanocage-encapsulated nanocrystals, Chem. Eur. J. 10 (2004) 3667–3672.

[8] S. Sayhan, A. Kınal, Stability of endohedral hydrogen doped boron nitride nanocages: a density functional theory study, Asian J. Chem. 26 (18) (2014) 5935–5939.

[9] R. Ahmadi, E.S. Mirkamali, Determination of thermodynamic parameters of produced materials from (ATTz) with boron nitride nano-cages in different conditions of temperature, with DFT method, J. Phys. Theor. Chem. 13 (3) (2016) 297–302.

[10] Maria; J. Iqbal, K. Ayub, Enhanced electronic and non-linear optical properties of alkali metal (Li, Na, K) doped boron nitride nano-cages. *Journal of Alloys and Compounds* 687 2016 976-983.

[11] Z. Slanina, M.-L. Sun, S.-L. Lee, Computations of boron and boron-nitrogen cages, Nano Struct. Mater. 8 (5) (1997) 623–635.

[12] P.P. Edwards, V.L. Kuznetsov, W.I.F. David, Hydrogen energy, Phil. Trans. R. Soc. A 365 (2007) 1043–1056.

[13] S. Sayhan, A. Kınal, Computational investigation of hydrogen storage capacity of boron nitride nanocages by newly developed PM7 method, Asian J. Chem. 27 (2015) 667–670.

[14] B.S. Okan, Z.Ö. Kocabaş, A.N. Ergün, M. Baysal, I. Letofsky-Papts, Y. Yürüm, Effect of reaction temperature and catalyst type on the formation of boron nitride nanotubes by chemical vapor deposition and measurement of their hydrogen storage capacity, Ind. Eng. Chem. Res 51 (2012) 11341–11347.

[15] T. Oku, M. Kuno, I. Narita, Hydrogen storage in boron nitride nanomaterials studied by TG/DTA and cluster calculation, J. Phys. Chem. Solids 65 (2004) 549–552.

[16] M.R.S.A. Janjua, Theoretical framework for encapsulation of inorganic $B_{12}N_{12}$ nanoclusters with alkaline earth metals for efficient hydrogen adsorption: a step forward toward hydrogen storage materials, Inorg. Chem. 60 (2021) 2816–2828.

[17] L. Goerigk, A. Hansen, C. Bauer, S. Ehrlich, A. Najibi, S. Grimme, A look at the density functional theory zoo with the advanced GMTKN55 database for general main group thermochemistry, kinetics and noncovalent interactions, Phys. Chem. Chem. Phys. 19 (2017) 32184.

[18] N. Mardirossian, M. Head-Gordon, Thirty years of density functional theory in computational chemistry: an overview and extensive assessment of 200 density functionals, Mol. Phys. 115 (19) (2017) 2315–2372.

[19] A. Karton, P.R. Spackman, Evaluation of density functional theory for a large and diverse set of organic and inorganic equilibrium structures, J. Comput. Chem. 42 (2021) 1590–1601.

[20] GaussView, Version 6, Dennington, Roy; Keith, Todd A.; Millam, John M. Semichem Inc., Shawnee Mission, KS, 2016.

[21] Gaussian 09, Revision D.01, Frisch, M. J.; Trucks, G. W.; Schlegel, H. B.; Scuseria, G. E.; Robb, M. A.; Cheeseman, J. R.; Scalmani, G.; Barone, V.; Petersson, G. A.; Nakatsuji, H.; Li, X.; Caricato, M.; Marenich, A. V.; Bloino, J.; Janesko, B. G.; Gomperts, R.; Mennucci, B.; Hratchian, H. P.; Ortiz, J. V.; Izmaylov, A. F.; Sonnenberg, J. L.; Williams-Young, D.; Ding, F.; Lipparini, F.; Egidi, F.; Goings, J.; Peng, B.; Petrone, A.; Henderson, T.; Ranasinghe, D.; Zakrzewski, V. G.; Gao, J.; Rega, N.; Zheng, G.; Liang, W.; Hada, M.; Ehara, M.; Toyota, K.; Fukuda, R.; Hasegawa, J.; Ishida, M.; Nakajima, T.; Honda, Y.; Kitao, O.; Nakai, H.; Vreven, T.; Throssell, K.; Montgomery, J. A., Jr.; Peralta, J. E.; Ogliaro, F.; Bearpark, M. J.; Heyd, J. J.; Brothers, E. N.; Kudin, K. N.; Staroverov, V. N.; Keith, T. A.; Kobayashi, R.; Normand, J.; Raghavachari, K.; Rendell, A. P.; Burant, J. C.; Iyengar, S. S.; Tomasi, J.; Cossi, M.; Millam, J. M.; Klene, M.; Adamo, C.; Cammi, R.; Ochterski, J. W.; Martin, R. L.; Morokuma, K.; Farkas, O.; Foresman, J. B.; Fox, D. J. Gaussian, Inc., Wallingford CT, 2009.

[22] Gaussian 16, Revision B.01, Frisch, M. J.; Trucks, G. W.; Schlegel, H. B.; Scuseria, G. E.; Robb, M. A.; Cheeseman, J. R.; Scalmani, G.; Barone, V.; Petersson, G. A.; Nakatsuji, H.; Li, X.; Caricato, M.; Marenich, A. V.; Bloino, J.; Janesko, B. G.; Gomperts, R.; Mennucci, B.; Hratchian, H. P.; Ortiz, J. V.; Izmaylov, A. F.; Sonnenberg, J. L.; Williams-Young, D.; Ding, F.; Lipparini, F.; Egidi, F.; Goings, J.; Peng, B.; Petrone, A.; Henderson, T.; Ranasinghe, D.; Zakrzewski, V. G.; Gao, J.; Rega, N.; Zheng, G.; Liang, W.; Hada, M.; Ehara, M.; Toyota, K.; Fukuda, R.; Hasegawa, J.; Ishida, M.; Nakajima, T.; Honda, Y.; Kitao, O.; Nakai, H.; Vreven, T.; Throssell, K.; Montgomery, J. A., Jr.; Peralta, J. E.; Ogliaro, F.; Bearpark, M. J.; Heyd, J. J.; Brothers, E. N.; Kudin, K. N.; Staroverov, V. N.; Keith, T. A.; Kobayashi, R.; Normand, J.; Raghavachari, K.; Rendell, A. P.; Burant, J. C.; Iyengar, S. S.; Tomasi, J.; Cossi, M.; Millam, J. M.; Klene, M.; Adamo, C.; Cammi, R.; Ochterski, J. W.; Martin, R. L.; Morokuma, K.; Farkas, O.; Foresman, J. B.; Fox, D. J. Gaussian, Inc., Wallingford CT, 2016.

[23] PerkinElmer, 2016. ChemBioDraw Ultra Version (15.1.0.144), CambridgeSoft Waltham, MA, USA.

[24] J.P. Perdew, K. Burke, M. Ernzerhof, Generalized gradient approximation made simple, Phys. Rev. Lett. 77 (1996) 3865–3868.

[25] J.P. Perdew, K. Burke, M. Ernzerhof, Errata: Generalized gradient approximation made simple, Phys. Rev. Lett. 78 (1997 1396.).

[26] C. Adamo, V. Barone, Toward reliable density functional methods without adjustable parameters: The PBE0 model, J. Chem. Phys. 110 (1999) 6158–6169.

[27] A.D. McLean, G.S. Chandler, Contracted Gaussian-basis sets for molecular calculations. 1. 2nd row atoms, Z=11-18, J. Chem. Phys. 72 1980 5639-5648.

[28] K. Raghavachari, J.S. Binkley, R. Seeger, J.A. Pople, Self-Consistent Molecular Orbital Methods. 20. Basis set for correlated wave-functions, J. Chem. Phys. 72 (1980) 650–654.

[29] C. Peng, H.B. Schlegel, Combining synchronous transit and quasi-newton methods for finding transition states, Israel J. Chem. 33 (1993) 449–454.

[30] Z. Slanina, M.L. Sun, S.L. Lee, Computations of boron and boron-nitrogen cages, Nano Structured Materials 8 (1997) 623–635.

[31] J. Li, L. Gao, Preparation of h-BN nano-film coated a-Si3N4 composite particles by a chemical route, J. Mater. Chem. 13 (2003) 628–630.

[32] R. Kumar, D. Raut, I. Ahmad, U. Ramamurty, T.K. Maji, C.N.O. Rao, Functionality preservation with enhanced mechanical integrity in the nanocomposites of the metal–organic framework, ZIF-8, with BN nanosheets, Mater. Horiz. 1 (2014) 513–517.

[33] G. Frenkin, H.F. Schaefer, The nature of the boron-carbon double bond in 2,4-diboramethylenecyclopropane, Chem. Phys. Lett. 109 (1984) 521–524.

[34] B. Glaser, H. Nöth, 9-Fluorenylidene-2,2,6,6-tetramethylpiperidinoborane: an allene isoester with two-coordinated boron and B=C double bond, Angew. Chem. Int. Ed. Engl. 24 (1985) 416–417.

[35] T.C. Bruice, F.C. Lightstone, Ground state and transition state contributions to the rates of intramolecular and enzymatic reactions, Acc. Chem. Res. 32 (2) (1999) 127–136.

[36] R.H. Higgins, Animation of imaginary frequencies at the transition state, J. Chem. Educ. 72 (8) (1995) 703.